

## Original Article

# Characterization of *NOL7* Gene Point Mutations, Promoter Methylation, and Protein Expression in Cervical Cancer

Colleen L. Doçi, Ph.D., Tanmayi P. Mankame, M.S., Alexander Langerman, M.D., Kelly R. Ostler, B.A., Rajani Kanteti, Ph.D., Timothy Best, B.S., Kenan Onel, M.D., Ph.D., Lucy A. Godley, M.D., Ph.D., Ravi Salgia, M.D., Ph.D., and Mark W. Lingen, D.D.S., Ph.D.

**Summary:** *NOL7* is a putative tumor suppressor gene localized to 6p23, a region with frequent loss of heterozygosity in a number of cancers, including cervical cancer (CC). We have previously demonstrated that reintroduction of *NOL7* into CC cells altered the angiogenic phenotype and suppressed tumor growth *in vivo* by 95%. Therefore, to understand its mechanism of inactivation in CC, we investigated the genetic and epigenetic regulation of *NOL7*. *NOL7* mRNA and protein levels were assessed in 13 CC cell lines and 23 consecutive CC specimens by real-time quantitative polymerase chain reaction, western blotting, and immunohistochemistry. Methylation of the *NOL7* promoter was analyzed by bisulfite sequencing and mutations were identified through direct sequencing. A CpG island with multiple CpG dinucleotides spanned the 5' untranslated region and first exon of *NOL7*. However, bisulfite sequencing failed to identify persistent sites of methylation. Mutational sequencing revealed that 40% of the CC specimens and 31% of the CC cell lines harbored somatic mutations that may affect the *in vivo* function of *NOL7*. Endogenous *NOL7* mRNA and protein expression in CC cell lines were significantly decreased in 46% of the CC cell lines. Finally, immunohistochemistry demonstrated strong *NOL7* nucleolar staining in normal tissues that decreased with histologic progression toward CC. *NOL7* is inactivated in CC in accordance with the Knudson 2-hit hypothesis through loss of heterozygosity and mutation. Together with evidence of its *in vivo* tumor suppression, these data support the hypothesis that *NOL7* is the legitimate tumor suppressor gene located on 6p23.  
**Key Words:** *NOL7*—Hypermethylation—Mutation.

From the Departments of Pathology, Medicine and Radiation and Cellular Oncology (C.L.D., T.P.M., M.W.L.); Surgery (A.L.), Section of Otolaryngology-Head and Neck Surgery; Medicine (K.R.O., R.K., L.A.G., R.S.), Section of Hematology/Oncology; and Pediatrics (T.B., K.O.), University of Chicago, Chicago, IL.

This study was supported in part by the Illinois Department of Public Health Penny Seaverns Cancer Research Fund (M.W.L.) and National Institutes for Health 5R01CA100750-07 (R.S.) and 5R01CA129501-03 (R.S.).

The authors declare no conflict of interest.

Address correspondence and reprint requests to Mark W. Lingen, Department of Pathology, University of Chicago, 5841 S. Maryland Avenue MC6101, Chicago, IL 60637. E-mail: mark.lingen@uchospitals.edu

Supplemental Digital Content is available for this article. Direct URL citations appear in the printed text and are provided in the HTML and PDF versions of this article on the Journal's Website, www.intjgynpathology.com.

Cervical cancer (CC) is the most common gynecological malignancy and the third most common cancer among women worldwide (1). CC development is strongly associated with human papillomavirus (HPV) infection. However, additional genetic alterations are required for malignant transformation (2–6). Therefore, the successful screening, prevention, diagnosis, and treatment of CC require further characterization of the key genetic alterations required for CC development. *NOL7* is a putative tumor suppressor gene (TSG) localized to 6p23, a region with frequent loss of heterozygosity (LOH) in a number of cancers, including hormone-refractory breast carcinoma, leukemia, lymphoma, osteosarcoma,

retinoblastoma, nasopharyngeal carcinoma, and CC (7–25). Using CC as a model, in which LOH of 6p23 is one of the most common allelic losses in this neoplasm (26–31), we demonstrated that *NOL7* expression is regulated through genomic instability. Fluorescent in-situ hybridization experiments using BAC clones and an 8-kb *NOL7* genomic probe demonstrated consistent loss of one *NOL7* allele in CC cell lines and in CC tumor samples (32). Reintroduction of *NOL7* into CC cells with decreased *NOL7* expression modulated the angiogenic phenotype by decreased expression of the proangiogenic cytokine vascular endothelial growth factor and increased expression of the antiangiogenic factor TSP-1. Importantly, reintroduction of *NOL7* suppressed tumor growth *in vivo* by 95% (32).

These studies suggest that *NOL7* plays a significant role in the suppression of tumor growth. However, according to the Knudson 2-hit hypothesis, inactivation of a TSG requires the functional loss of both alleles through various genetic or epigenetic mechanisms (33,34). Although numerous studies, including those within our own lab, have documented the LOH of 6p23 and *NOL7*, an additional hit has not been identified. In addition to the LOH, mutation and methylation represent 2 common methods of genetic and epigenetic inactivation (35,36). A recent study identified mutations within *NOL7* in 25% of the CC specimens examined. However, the limited number of samples investigated precludes definitive conclusions (37). Promoter methylation of genes localized to 6p is associated with cancer, and methylation of *ID4* and *POU2F3* has been reported on 6p23 (38,39). However, no studies have specifically determined the methylation status of *NOL7*.

## MATERIALS AND METHODS

### Identification of GC-rich Genomic Regions and CpG Islands

The EMBOSS-Isochore program was used to identify regions within the *NOL7* gene that were GC rich (40–42). The program was input with base pairs 13,614,790 to 13,621,437 of the Chr6 Genbank accession NC\_000006.11. This identified a region from 13,614,790 to 13,616,240, which was subsequently analyzed for CpG islands using the EMBOSS-CpGPlot program (43,44). Default settings for both programs were used (GC > 0.5 and CpG > 0.7 thresholds).

### Cell Lines

All cell lines were obtained from the ATCC (Manassas, VA) and were cultured at 37°C in a 5% CO<sub>2</sub> in humidified incubators. Media and reagents were purchased from Invitrogen (Carlsbad, CA). HEK293 T was used as a positive control for *NOL7* expression. All media were supplemented with 10% FBS, penicillin (100 µg/mL), and streptomycin. Media were as follows: SiHa, Ca Ski, and ME180—RPMI; HeLa and HEK293 T—DMEM; AN3CA, C-33A, MS751, and CC-I—MEM; HEC-1-A and HT-3—McCoy's; C-4I and C-4II—Waymouth's; and SW756—Leibovitz's. Genomic DNA from cell lines was extracted using the Gentra Puregene Kit (Qiagen, Valencia, CA) as per the manufacturer's instructions. Genomic DNA from normal adult cervix was obtained from the Biochain Institute Incorporated (Hayward, CA).

### Tissue Specimens

CC tissue specimens were collected and used under the approval of the University of Chicago Institutional Review Board. Paraffin blocks of diagnosed CC specimens were obtained and representative hematoxylin and eosin-stained sections were reviewed. Matched normal and cancer specimens were collected by laser capture microdissection) using the Leica AS LMD system. Genomic DNA from laser capture microdissection sections was extracted as described previously (45).

### Bisulfite Treatment and Polymerase Chain Reaction Amplification

Genomic DNA from the cell lines, normal cervical mucosa, and 23 CC samples were treated with sodium bisulfite as described previously (46). The bisulfite-treated DNA was used as template for polymerase chain reaction (PCR), using AmpliTaq Gold PCR Master Mix (Applied Biosystems, Foster City, CA) and primers region A (5'-GTGGTAGTAGGGTTG ATTGG-3' and 5'-AATAAACCCCACTAAAAAT ACTCTAC-3') and region B (5'-GTAGAGTATTTT TAGTGGGGTTTATT-3' and 5'-AAACTACACCA TAACCCA-3') (Figure 4). The PCR program used was 94°C for 10 minutes, 35 cycles of 94°C for 30s, 59°C for 45s, 72°C for 45s, and 72°C for 10 minutes. The PCR products were resolved and visualized on a 1% agarose gel.

### TOPO TA Cloning and Sequencing

PCR products from bisulfite-treated DNA extracted from cell lines and tissue samples were cloned into the pCR4-TOPO vector by TOPO TA cloning according to the manufacturer's instructions (Invitrogen, Carlsbad, CA). Ten colonies per transformation were sequenced using T7 and T3 primer sites within the pCR4-TOPO vector. Sequences were compared with the genomic template (accession number: NC\_000006.11) and the CpGs were analyzed using MegAlign software (DNASTAR, Inc., Madison, WI).

### Mutational Sequencing

Genomic DNA from cell lines and tissues was amplified by PCR using AmpliTaq Gold PCR Master Mix (Applied Biosystems). Primers are listed in Supplementary Table 1 (Table, Supplemental Digital Content 1; <http://links.lww.com/IJGP/A6>). Cycling conditions were 94°C for 5 minutes, 35 cycles of 94°C for 20 seconds, varied  $T_m$  for 30 seconds, 72°C for 2 minutes, and 72°C for 10 minutes. PCR products were purified using the Wizard SV Gel and PCR Cleanup System (Promega, Madison, WI) and sequenced using amplification primers. Sequences were compared with bases 13,614,022 to 13,621,437 of NC\_000006.11 using MegAlign software (DNASTAR, Inc.) and ChromasLite (Technelysium Pty Ltd, Eden Prairie, MN). Potential biologic significance of the mutations was evaluated using Genomatix MatInspector (47), Human Splicing Finder (48), CRYP-SKIP (49–51), MicroInspector Prediction Software (52), and miRBase (53–57).

### Real-Time Quantitative PCR

Endogenous NOL7 mRNA expression was determined by quantitative real-time PCR as described previously (58). Relative fold change for mRNA expression was quantified using the  $\Delta\Delta C_T$  relative quantification method and normalized to 293T mRNA levels. Statistical significance was determined using the Student *t* test.

### Western Blotting

Western blotting was performed as described (58). Antibody conditions were as follows: NOL7 (12 ng/mL) (Sigma-Aldrich, St. Louis, MO);  $\beta$ -actin (0.75 ng/mL) (Abcam, Cambridge, MA); and goat  $\alpha$ -rabbit-HRP (12.5 ng/mL) (Cell Signaling Technology, Danvers, MA). Results were quantified using

the Bio-Rad QuantityOne Software (Bio-Rad, Hercules, CA) and normalized to  $\beta$ -actin.

### Tissue Microarray and Immunohistochemistry

Immunohistochemistry for NOL7 was performed on cervical tissue obtained with the approval of the University of Chicago Institutional Review Board. A tissue microarray (TMA) was generated using a Beecher Instruments ATA-27 Automated Tissue Arrayer. The TMA consisted of normal cervical mucosa (n = 70), cervical intraepithelial neoplasia (CIN) I (n = 22), CIN II (n = 20), CIN III (n = 23), and cervical squamous cell carcinoma (n = 88). Deparaffinized sections were microwaved in ET buffer,  $\alpha$ -NOL7 primary (Sigma-Aldrich) was applied at 1:120 dilution for 1 hour at room temperature, and the rabbit EnVision + kit (DAKO, Carpinteria, CA) was used for detection. All sections were counterstained with hematoxylin and scored on a 0 to 2+ scale, with 0 being the lowest staining and 2+ the greatest. The Fisher exact test was performed for the comparison of NOL7 expression among the histologic groups. Unless otherwise stated, NOL7 expression was ranked as present (staining intensity 1 and 2) or absent (staining intensity 0) against normal + CIN I versus CIN II + CIN III + squamous cell carcinoma (SCC) groups.

## RESULTS

NOL7 is downregulated in CC cell lines and its expression decreases with progression in CC. We have previously demonstrated decreased mRNA expression and allelic loss of *NOL7* in a limited number of CC cell lines and tumor samples by Northern blot and fluorescent in-situ hybridization (32). To further characterize the expression of endogenous NOL7 in CC, we assessed mRNA and protein levels in an expanded set of CC cell lines. Using a polyclonal antibody against NOL7, we performed western blotting (Fig. 1A) and compared this with mRNA levels as determined by real-time quantitative PCR (Fig. 1B), normalized to 293 T cells for which previous analyses have indicated as containing high levels of endogenous normal NOL7. NOL7 protein expression was decreased by half in 6 of 13 (46%) cell lines compared with 293 T control (Fig. 1A). We also found that 6 of 13 (46%) CC cell lines demonstrated significantly decreased NOL7 mRNA expression (<50% of 293 T control,

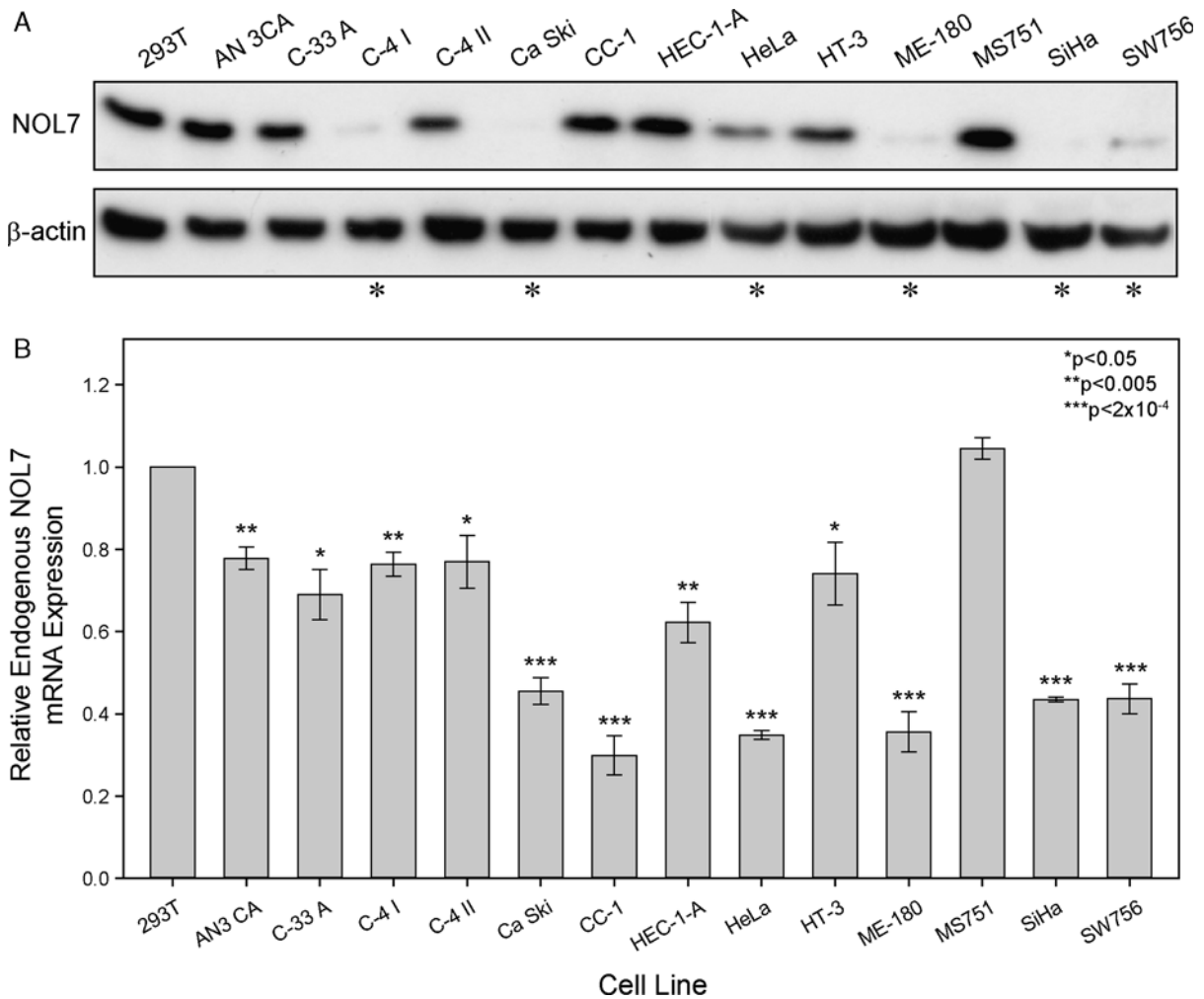


**FIG. 1.** Analysis of endogenous NOL7 expression in CC cell lines. (A) Western blotting was performed on 25  $\mu$ g of whole cell lysate from a panel of CC cell lines. Expression was quantified in (B) using QuantityOne software from Bio-Rad and normalized to  $\beta$ -actin. (B) Real-time quantitative polymerase chain reaction was performed on total RNA isolated from 13 CC cell lines and compared with 293T controls.

$P < 2 \times 10^{-4}$ ; Fig. 1B). Four of these cell lines, Ca Ski, ME-180, SiHa, and SW756, demonstrated consistently downregulated NOL7 mRNA and protein. Interestingly, 5 of the 13 (40%) cell lines, C-4 I, Ca Ski, CC-1, HEC-1-A, and HeLa, showed differential expression between NOL7 mRNA and protein levels, suggesting that NOL7 may also be posttranscriptionally and posttranslationally regulated.

To assess endogenous NOL7 expression during the histologic progression of CC, immunohistochemistry against NOL7 was performed on TMAs consisted of specimens from normal, CIN I, CIN II, CIN III, and SCC cervical tissue (Fig. 2A). Tissues were scored 0, 1, or 2 based on staining intensity, with 0 being the lowest and 2 being the highest expressing tissue. Although the majority (95%) of normal and CIN I samples

demonstrated staining for NOL7, <23% of samples from CIN II, CIN III, and SCC had a staining intensity of 1 or 2 ( $P < 0.001$ ) (Fig. 2B). Conversely, 77% of CIN II, CIN III, and SCC tissues did not express endogenous NOL7, whereas only 5% of normal and CIN I tissues lacked NOL7 expression ( $P < 0.001$ ) (Fig. 2B). These data suggest that NOL7 expression decreases significantly with histologic progression in CC, and that loss of NOL7 occurs after CIN I.

#### CC Cell Lines and Tumor Samples Do Not Have Methylated NOL7 Promoter

The significant loss of NOL7 expression in CC cell lines and cervical tissue suggests that NOL7 may function as a TSG. In accordance with the Knudson

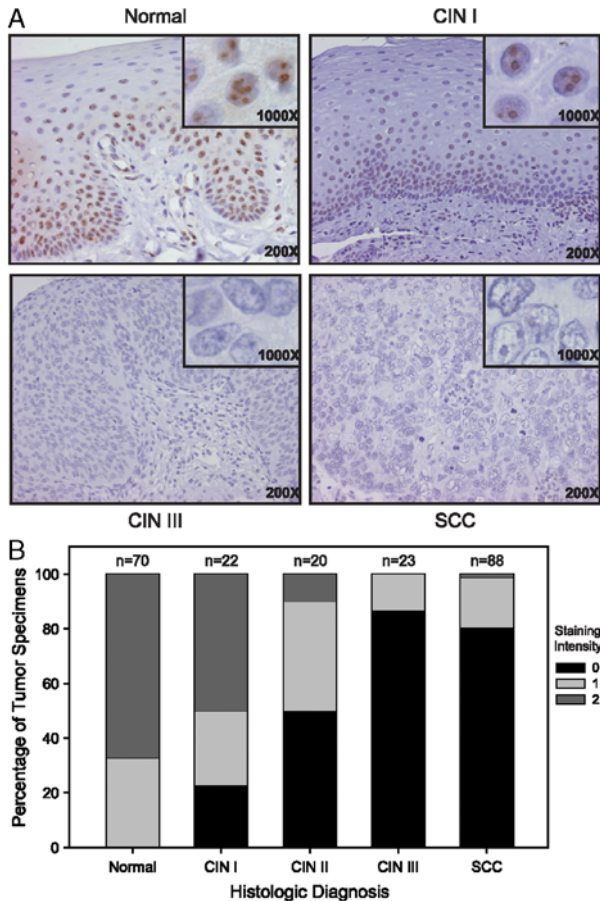


**FIG. 2.** Immunohistochemical expression of NOL7 in normal (A) CIN I (B) CIN III (C), and malignant cervical mucosa (D). Decreased nucleoplasmic NOL7 protein expression is observed with increasing histologic atypia. Original magnification: 200 $\times$  and 1000 $\times$ . E, Quantification of NOL7 expression in cervical mucosa. Normal (n = 70), CIN I (n = 22), CIN II (n = 20), CIN III (n = 23), and SCC (n = 88). Data are expressed as percentage of tumor specimens demonstrating an intensity of staining ranging from 0 to 2+.

2-Hit hypothesis, loss of the first allele of *NOL7* by LOH must be followed by loss or silencing of the second allele through genetic or epigenetic mechanisms, likely methylation or mutation. Epigenetic regulation by methylation in a gene-specific manner is dictated by the presence of a CpG island in the promoter of these genes (59). To determine whether *NOL7* might be regulated by this mechanism, the *NOL7* genomic region was analyzed for high GC content that might indicate the presence of a CpG island. The region upstream of the *NOL7* start codon averages >60% GC across the region of interest (Fig. 3A) (40–42). To determine whether this GC-rich region contained a CpG island, the genomic region

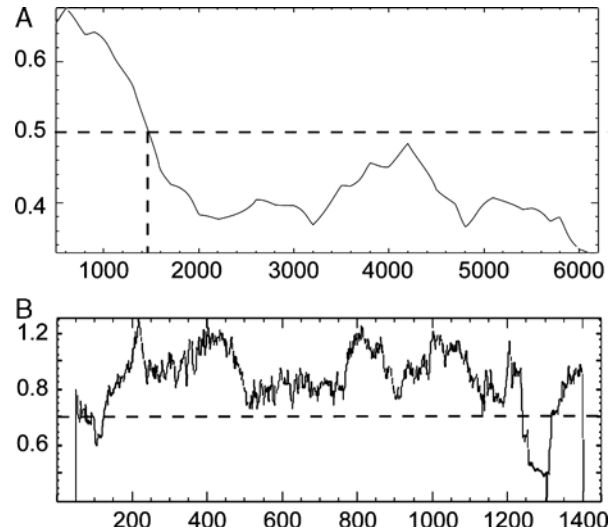


**FIG. 3.** Prediction and analysis of *NOL7* genomic elements. (A) The genomic region of chromosome 6 (NC\_000006.11) from bases 13,614,790 to 13,621,437 was analyzed using EMBOSS Isochore program to predict regions of high GC content. Dashed lines indicate the designated threshold of 0.5. (B) The 1451 bp region of *NOL7* demonstrating that >50% GC content was analyzed for the presence of a CpG island using EMBOSS CpGPlot. Dashed lines indicate a threshold of 0.7.

sequence was analyzed using the EMBOSS CpG Plot program (44,46). The analysis predicted a large CpG island approximately 1120 nucleotides in length, containing 111 CpG dinucleotides (Figs. 3B).

Promoter hypermethylation is a common mechanism by which many TSGs such as p16 and APC are silenced in CC (60). The promoter of *NOL7* spans the 560 bp region upstream of the start codon, which contains 47 CpG dinucleotides (58). To specifically assess *NOL7* promoter methylation, bisulfite PCR primers were designed such that the promoter region was split into 2 fragments, region A and B (Fig. 4A). To assess the methylation status of *NOL7* in cell lines that express a wide spectrum of endogenous *NOL7*, genomic DNA from 293 T, HeLa, and SiHa cell lines that express high, moderate, and low levels of endogenous *NOL7* was bisulfite treated, PCR amplified, and TOPO TA cloned (Fig. 4B). There was no methylation observed in the 3 cell lines (Fig. 4C). To determine whether the lack of methylation was an artifact due to cell culture, 23 consecutive CC tissue samples were analyzed and compared with normal cervix for methylation status. No significant methylation pattern was observed in either the normal or CC tissue samples (Fig. 4C). These data suggest that methylation is not a mechanism of inactivation of the *NOL7* gene.

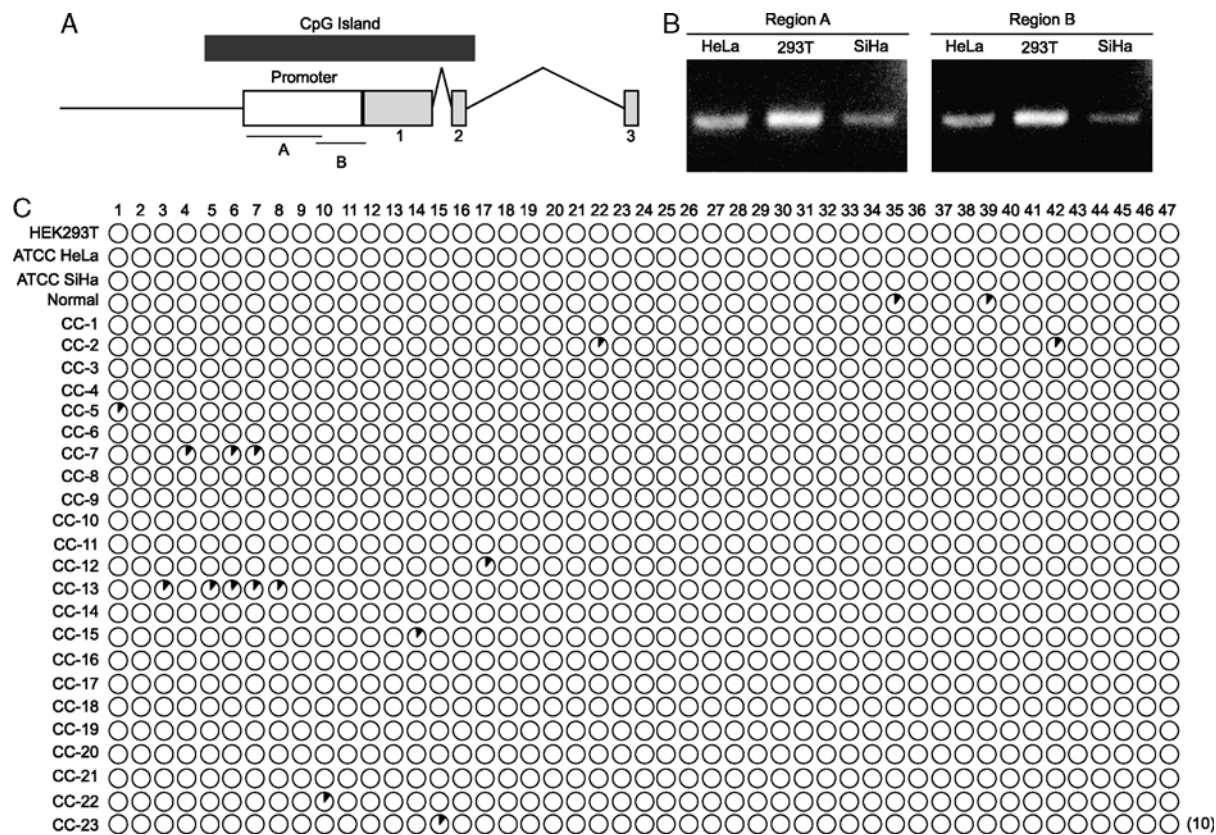


**FIG. 4.** Bisulfite PCR-mediated methylation analysis. (A) Schematic of the *NOL7* genomic region with exons (light gray box), promoter region (white box), and CpG Island (dark gray box). (A) and (B) indicate the bisulfite primer location. (B) Representative bisulfite polymerase chain reaction products for regions A and B from HEK293 T, HeLa, and SiHa cell lines. (C) Analysis of the methylation pattern of 47 individual CpG dinucleotides in the *NOL7* promoter region. Ten clones were sequenced for the 3 cell lines, normal, and 23 cervical cancer samples (CC-1 to 23), which is represented in parentheses. Open circles represent unmethylated CpG dinucleotides. Ten clones are represented per circle, with the methylated CpGs corresponding to the black shaded fraction.

### ***NOL7* is Mutated in CC**

Lack of *NOL7* methylation in the promoter region suggested that there may be inactivation through mutation. To determine whether the genomic region of *NOL7* harbors inactivating mutations, a series of primers were designed to cover the length of the

*NOL7* gene. Genomic DNA from cell lines (Table 1) and 23 consecutive matched normal and CC tumor specimens (Table 2) were collected and the *NOL7* genomic region was sequenced. Four consistent variations from the genomic sequence of *NOL7* were identified within the 13 cell lines. Fifteen of the 23

**TABLE 1.** Mutational analysis of *NOL7* genomic region in CC cell lines

Variance	Genomic	<i>NOL7</i> region	Coding change	SNP	Frequency	Predicted biologic consequence
A → C	13615401	Promoter		rs2841524	61.54%	HIF1 $\alpha$ -binding site lost
G → A	13615702	Exon 1	G38R	—	61.54%	May affect functionality of adjacent acidic domain
G → A	13618408	Intron 5		—	38.46%	Destroys splicing silencer motifs and creates new enhancer motifs; alternative splicing pattern
T → C	13620097	Intron 5		—	7.69%	Destroys splicing silencer motifs and creates new enhancer motifs; alternative splicing pattern

The results of direct mutational sequencing of the *NOL7* genomic region within CC cell lines are listed. The location of the mutation corresponding to Genbank accession NC\_000006.11 is listed, along with the region of *NOL7* affected and frequency of the mutation within the 13 cell lines examined. The mutation, SNP status, and predicted effect are included. CC indicates cervical cancer.

**TABLE 2.** Mutational analysis of NOL7 genomic region in CC tumor samples

Variance	Genomic	NOL7 region	SNP	Frequency	Predicted biologic consequence
G → A	13614430	5' UTR	—	4.35%	Loss of hsa-miR-1225-3p, -145, -331-3p, -1274a, -500, and -326; Gain of hsa-miR-134
A → C	13615401	Promoter	rs2841524	39.13%	HIF1 $\alpha$ -binding site lost
C → T	13615444	Promoter	—	4.35%	AP-2-binding site lost
G → A	13617979	Intron 3	—	4.35%	Destroys splicing silencer and enhancer motifs; splice site broken
A → G	13618177	Intron 4	—	4.35%	Destroys splicing silencer motifs and creates new enhancer motifs; alternative splicing pattern
G → A	13618408	Intron 5	—	8.70%	Destroys splicing silencer motifs and creates new enhancer motifs; alternative splicing pattern
T → C	13620207	Intron 5	—	4.35%	Destroys splicing silencer and enhancer motifs; splice site broken
A → G	13620386	Intron 5	—	4.35%	Destroys splicing silencer and enhancer motifs; splice site broken
+AACT	13621391	3'UTR	rs10695200	4.35%	Change in 3' UTR cis-elements
Deletion	13621627	3'UTR	—	4.35%	Loss of hsa-miR-19-1b and -182;Gain of hsa-miR-1184
G → A	13621698	3'UTR	—	4.35%	Loss of hsa-miR-106b;Gain of hsa-miR-548m

The results of direct mutational sequencing of the NOL7 genomic region in CC tumor samples are listed. The location of the mutation corresponding to Genbank accession NC\_000006.11 is listed, along with the region of NOL7 affected. The mutation, SNP status, and predicted effect are included. The total mutation frequency is indicated.

samples showed variation from the National Center for Biotechnology Information reference sequence, and 40% of these represented somatic tumor-associated mutations. The majority of these mutations are clustered in intron 5 and the 3' untranslated region (UTR) of NOL7. One mutation in intron 5 was identified in 2 of the tumor samples and in 5 of the 13 cell lines examined (G13618408A). Using software prediction programs, the majority of the intronic mutations are within splicing regions that may influence alternative splicing of the NOL7 gene, whereas the 3' UTR mutations are associated with multiple miRNA sites (Tables 1, 2). In addition to somatic tumor-associated mutations, some cell lines and tumor samples also demonstrated single-nucleotide polymorphism (SNP) variations. In particular, SNP rs2841524 is located in the promoter region of NOL7. The variation at this locus was identified in 61% of CC cell lines and 39% of tumor samples. Variation of this particular allele from A → C is predicted to change the consensus HIF-1 $\alpha$ -binding element within the promoter. Taken together, this demonstrates that NOL7 harbors tumor-associated mutations and SNP variations, and suggests these genomic alterations may potentially contribute to NOL7 inactivation in conjunction with LOH.

**DISCUSSION**

HPV infection has a well-characterized role in the pathogenesis of CC (61–63). However, this event is

insufficient for oncogenesis, and the genetic and epigenetic changes that contribute to the development of CC are poorly understood. Chromosomal instability and LOH were among the first nonviral mechanisms identified that contribute to CC (26–29,64). However, a limited number of putative TSGs, and their functional role in the development of CC, have been adequately described. One of the most common allelic losses in CC occurs at 6p23 (26–31). Within this chromosomal region, there are several potential cancer-associated genes, including CD83 and NOL7. Evidence of genetic alterations of CD83 in CC has been demonstrated (37,65). However, functional demonstration of its tumor suppressive capacity is lacking. Conversely, we have previously shown that NOL7 displays allelic loss in both CC cell lines and tumor samples. Furthermore, reintroduction of NOL7 into CC tumor cell lines suppresses *in vivo* tumor growth by 95% in part by the modulation of the angiogenic phenotype (32). In this study, we investigated the genetic and epigenetic regulation of NOL7 and provide evidence of both mutations and LOH, further supporting the role of NOL7 as a TSG in CC.

CC development represents a continuum of cytologic and molecular alterations that occurs over decades. The interrogation of normal cervical mucosa and various grades of CIN and CC demonstrated a decrease in the number of samples demonstrating NOL7 protein expression at the juncture between CIN I and CIN II (77.3% and 50.0%; Fig. 2B). A further decrease was observed in CIN III (13%,

Fig. 2B) and vast majority of CC lacked *NOL7* expression (19.3%; Fig. 2B). This mirrors the progressive gain of expression of the angiogenic phenotype, as measured by the surrogate of microvessel density, during CC development (66–72). Interestingly, the dramatic loss of *NOL7* expression in CIN III also correlates with the stable integration of the HPV E6 and E7 oncoproteins (62,73,74). Therefore, decreased *NOL7* expression concurrent with increased microvessel density and HPV integration supports the hypothesis that loss of *NOL7* plays a critical role in the expression of the angiogenic phenotype during CC development and suggests that *NOL7* expression may be additionally regulated through HPV oncoproteins. Although it is currently unknown whether there is a direct correlation between HPV type and *NOL7* expression levels, the impact of HPV oncoproteins on upstream regulation of *NOL7* is being investigated. It will also be of interest to determine whether other cancers whose etiology is correlated with HPV infection, such as head and neck cancers, also demonstrate differential expression of *NOL7* during histologic progression as has been observed in our CC model system.

Both global DNA hypomethylation and regional DNA hypermethylation have been observed in CC, suggesting that methylation is likely a key mechanism for regulation of gene expression in CC (75). The identification of a CpG island within the promoter region of *NOL7* suggested that the expression of the *NOL7* gene might be epigenetically regulated. However, no methylation was detected in cell lines or tumor samples, suggesting that methylation is not a mechanism of *NOL7* regulation. In addition to the promoter region CpG island, an additional CpG island within the fifth intron of the *NOL7* gene was detected. Although nonpromoter methylation has been described in gene bodies and intergenic regions, their functional significance is not well understood (76,77). Nonpromoter methylation can enhance transcription in a protein-specific and tissue-specific manner (78). Enhanced methylation in intergenic regions is also associated with splicing efficiency (79). A number of mutations were also detected in this region, suggesting that intron 5 may be an epigenetic hotspot that is targeted during CC development.

The mutations identified within intron 5 and other introns are predicted to affect splicing patterns of the flanking exons. Alternative splicing may account for up to 75% of the diversity in the human proteome and it is estimated that as much as 15% of the

somatic mutations in cancer are attributable to alternative splicing (80,81). These alternative splicing patterns can manifest as truncated, frameshifted, or unstable transcripts. Alternative or truncated protein products would likely demonstrate altered functionality *in vivo*, as critical localization domains of *NOL7* are coded within the carboxy terminus of the protein (82). Aberrant splicing patterns can also negatively impact the stability and expression of mutant transcripts, triggering nonsense-mediated decay and other nuclear surveillance mechanisms (83–85). In addition, coupled splicing mechanisms can lead to altered cotranscriptional processing, leading to differential expression of an mRNA at multiple levels (86–88). Mutations within the 3' UTR of genes have also been shown to have significant effects on mRNA polyadenylation, stability, export, and subsequent translation (89–91). Although the effect of the specific mutations on *NOL7* expression and function cannot be determined from this study alone, the number of mutations within a small genomic locus suggests that *NOL7* may play a critical role in CC development and progression. It will be critical to experimentally determine the effect of these genetic alterations on *NOL7* isoform expression, and to assess their functional consequences in the context of the second *NOL7* allele. In addition, some of the identified nucleotide changes correlate with characterized SNPs *NOL7*. In particular, the expression of the A versus C allele identified in the promoter region of *NOL7* corresponds to the consensus for an HIF-1 $\alpha$ -binding site. Although the role of HIF-1 $\alpha$  in *NOL7* expression must be validated experimentally, this is particularly compelling when considered in conjunction with data showing that loss of *NOL7* correlates with the onset of angiogenesis in CC clinical progression.

In conclusion, *NOL7* is a putative TSG in CC and perhaps other malignancies with loss of 6p23. In this study, we sought to characterize the expression of endogenous *NOL7* in CC and to identify the mechanism of inactivation of its other allele. *NOL7* was found to be significantly downregulated in 6 of 13 CC cell lines. Furthermore, *NOL7* protein expression decreased with histologic progression. Through bisulfite and mutational sequencing of CC cell lines and tumor samples, we demonstrated that *NOL7* is not methylated, but contains numerous tumor-associated somatic mutations and potentially deleterious SNPs in CC cell lines and tissue specimens. This provides additional evidence for the role of *NOL7* as a bona fide TSG in CC and suggests a mechanism by which *NOL7* may contribute to the pathogenesis of cancer.

## REFERENCES

1. Jemal A, Bray F, Center MM, et al. Global cancer statistics. *CA Cancer J Clin* 2011;61:69–90.
2. Narisawa-Saito M, Yoshimatsu Y, Ohno S, et al. An in vitro multistep carcinogenesis model for human cervical cancer. *Cancer Res* 2008;68:5699–705.
3. Branca M, Giorgi C, Ciotti M, et al. Down-regulated nucleoside diphosphate kinase nm23-H1 expression is unrelated to high-risk human papillomavirus but associated with progression of cervical intraepithelial neoplasia and unfavourable prognosis in cervical cancer. *J Clin Pathol* 2006;59:1044–51.
4. Kaufmann AM, Backsch C, Schneider A, et al. HPV induced cervical carcinogenesis: molecular basis and vaccine development. *Zentralbl Gynakol* 2002;124:511–24.
5. Walboomers JM, Jacobs MV, Manos MM, et al. Human papillomavirus is a necessary cause of invasive cervical cancer worldwide. *J Pathol* 1999;189:12–9.
6. Lazo PA. The molecular genetics of cervical carcinoma. *Br J Cancer* 1999;80:2008–18.
7. Lung ML, Choi CV, Kong H, et al. Microsatellite allelotyping of chinese nasopharyngeal carcinomas. *Anticancer Res* 2001;21:3081–4.
8. Liao SK, Perng YP, Shen YC, et al. Chromosomal abnormalities of a new nasopharyngeal carcinoma cell line (NPC-BM1) derived from a bone marrow metastatic lesion. *Cancer Genet Cytogenet* 1998;103:52–8.
9. Mutirangura A, Tanunyutthawongse C, Pornthanakasm W, et al. Genomic alterations in nasopharyngeal carcinoma: loss of heterozygosity and Epstein-Barr virus infection. *Br J Cancer* 1997;76:770–6.
10. Lim G, Karaskova J, Vukovic B, et al. Combined spectral karyotyping, multicolor banding, and microarray comparative genomic hybridization analysis provides a detailed characterization of complex structural chromosomal rearrangements associated with gene amplification in the osteosarcoma cell line MG-63. *Cancer Genet Cytogenet* 2004;153:158–64.
11. Takeshita A, Naito K, Shinjo K, et al. Deletion 6p23 and add(11)(p15) leading to NUP98 translocation in a case of therapy-related atypical chronic myelocytic leukemia transforming to acute myelocytic leukemia. *Cancer Genet Cytogenet* 2004;152:56–60.
12. Amare Kadam PS, Ghule P, Jose J, et al. Constitutional genomic instability, chromosome aberrations in tumor cells and retinoblastoma. *Cancer Genet Cytogenet* 2004;150:33–43.
13. Fan YS, Rizkalla K. Comprehensive cytogenetic analysis including multicolor spectral karyotyping and interphase fluorescence in situ hybridization in lymphoma diagnosis. a summary of 154 cases. *Cancer Genet Cytogenet* 2003;143:73–9.
14. Batanian JR, Cavalli LR, Aldosari NM, et al. Evaluation of paediatric osteosarcomas by classic cytogenetic and CGH analyses. *Mol Pathol* 2002;55:389–93.
15. Starostik P, Patzner J, Greiner A, et al. Gastric marginal zone B-cell lymphomas of MALT type develop along 2 distinct pathogenetic pathways. *Blood* 2002;99:3–9.
16. Giagounidis AA, Hildebrandt B, Heinsch M, et al. Acute basophilic leukemia. *Eur J Haematol* 2001;67:72–6.
17. Achuthan R, Bell SM, Roberts P, et al. Genetic events during the transformation of a tamoxifen-sensitive human breast cancer cell line into a drug-resistant clone. *Cancer Genet Cytogenet* 2001;130:166–72.
18. Shao JY, Wang HY, Huang XM, et al. Genome-wide allelotyping analysis of sporadic primary nasopharyngeal carcinoma from southern China. *Int J Oncol* 2000;17:1267–75.
19. Chen Z, Issa B, Brothman LJ, et al. Nonrandom rearrangements of 6p in malignant hematological disorders. *Cancer Genet Cytogenet* 2000;121:22–5.
20. Nakase K, Wakita Y, Minamikawa K, et al. Acute promyelocytic leukemia with del(6)(p23). *Leuk Res* 2000;24:79–81.
21. Nagai H, Kinoshita T, Suzuki H, et al. Identification and mapping of novel tumor suppressor loci on 6p in diffuse large B-cell non-Hodgkin's lymphoma. *Genes Chromosomes Cancer* 1999;25:277–83.
22. Nemani M, Bellanne-Chantelot C, Cohen D, et al. Detection of triplet repeat sequences in yeast artificial chromosomes using oligonucleotide probes: application to the SCA1 region in 6p23. *Cytogenet Cell Genet* 1996;72:5–8.
23. Jadayel D, Calabrese G, Min T, et al. Molecular cytogenetics of chronic myeloid leukemia with atypical t(6;9) (p23;q34) translocation. *Leukemia* 1995;9:981–7.
24. Hoyle CF, Sherrington P, Hayhoe FG. Translocation (3;6)(q21;p21) in acute myeloid leukemia with abnormal thrombopoiesis and basophilia. *Cancer Genet Cytogenet* 1988;30:261–7.
25. Fleischman EW, Prigogina EL, Iljinskaja GW, et al. Chromosomal rearrangements with a common breakpoint at 6p23 in five cases of myeloid leukemia. *Hum Genet* 1983;64:254–6.
26. Mitra AB, Murty VV, Li RG, et al. Allelotype analysis of cervical carcinoma. *Cancer Res* 1994;54:4481–7.
27. Kersemaekers AM, Kenter GG, Hermans J, et al. Allelic loss and prognosis in carcinoma of the uterine cervix. *Int J Cancer* 1998;79:411–17.
28. Huettner PC, Gerhard DS, Li L, et al. Loss of heterozygosity in clinical stage IB cervical carcinoma: relationship with clinical and histopathologic features. *Hum Pathol* 1998;29:364–70.
29. Rader JS, Gerhard DS, O'Sullivan MJ, et al. Cervical intraepithelial neoplasia III shows frequent allelic loss in 3p and 6p. *Genes Chromosomes Cancer* 1998;22:57–65.
30. Rader JS, Li Y, Huettner PC, et al. Cervical cancer suppressor gene is within 1 cM on 6p23. *Genes Chromosomes Cancer* 2000;27:373–9.
31. Mullokandov MR, Kholodilov NG, Atkin NB, et al. Genomic alterations in cervical carcinoma: losses of chromosome heterozygosity and human papilloma virus tumor status. *Cancer Res* 1996;56:197–205.
32. Hasina R, Pontier AL, Fekete MJ, et al. NOL7 is a nucleolar candidate tumor suppressor gene in cervical cancer that modulates the angiogenic phenotype. *Oncogene* 2006;25:588–98.
33. Knudson AG Jr. Mutation and cancer: statistical study of retinoblastoma. *Proc Natl Acad Sci U S A* 1971;68:820–3.
34. Knudson AG. Two genetic hits (more or less) to cancer. *Nat Rev Cancer* 2001;1:157–62.
35. Hanahan D, Weinberg RA. The hallmarks of cancer. *Cell* 2000;100:57–70.
36. Herman JG, Baylin SB. Gene Silencing in Cancer in Association with Promoter Hypermethylation. *N Engl J Med* 2003;349:2042–54.
37. Zhang Z, Borecki I, Nguyen L, et al. CD83 gene polymorphisms increase susceptibility to human invasive cervical cancer. *Cancer Res* 2007;67:11202–8.
38. Hagiwara K, Nagai H, Li Y, et al. Frequent DNA methylation but not mutation of the ID4 gene in malignant lymphoma. *J Clin Exp Hematop* 2007;47:15–8.
39. Zhang Z, Huettner PC, Nguyen L, et al. Aberrant promoter methylation and silencing of the POU2F3 gene in cervical cancer. *Oncogene* 2006;25:5436–45.
40. Pesole G, Bernardi G, Saccone C. Isochore specificity of AUG initiator context of human genes. *FEBS Lett* 1999;464:60–2.
41. Bernardi G. Isochores and the evolutionary genomics of vertebrates. *Gene* 2000;241:3–17.
42. Bernardi G. The human genome: organization and evolutionary history. *Annu Rev Genet* 1995;29:445–76.
43. Gardiner-Garden M, Frommer M. CpG islands in vertebrate genomes. *J Mol Biol* 1987;196:261–82.
44. Rice P, Longden I, Bleasby A. EMBOS: the European Molecular Biology Open Software Suite. *Trends Genet* 2000;16:276–7.

45. Kanteti R, Yala S, Ferguson MK, et al. MET, HGF, EGFR, and PXN gene copy number in lung cancer using DNA extracts from FFPE archival samples and prognostic significance. *J Environ Pathol Toxicol Oncol* 2009;28:89–98.
46. Clark SJ, Harrison J, Paul CL, et al. High sensitivity mapping of methylated cytosines. *Nucleic Acids Res* 1994;22:2990–97.
47. Cartharius K, Frech K, Grote K, et al. MatInspector and beyond: promoter analysis based on transcription factor binding sites. *Bioinformatics* 2005;21:2933–42.
48. Desmet FO, Hamroun D, Lalande M, et al. Human Splicing Finder: an online bioinformatics tool to predict splicing signals. *Nucleic Acids Res* 2009;37:e67.
49. Kralovicova J, Vorechovsky I. Global control of aberrant splice-site activation by auxiliary splicing sequences: evidence for a gradient in exon and intron definition. *Nucleic Acids Res* 2007;35:6399–13.
50. Buratti E, Chivers M, Kralovicova J, et al. Aberrant 5' splice sites in human disease genes: mutation pattern, nucleotide structure and comparison of computational tools that predict their utilization. *Nucleic Acids Res* 2007;35:4250–63.
51. Vorechovsky I. Aberrant 3' splice sites in human disease genes: mutation pattern, nucleotide structure and comparison of computational tools that predict their utilization. *Nucleic Acids Res* 2006;34:4630–41.
52. Baev V, Daskalova E, Minkov I. Computational identification of novel microRNA homologs in the chimpanzee genome. *Comput Biol Chem* 2009;33:62–70.
53. Griffiths-Jones S. The microRNA Registry. *Nucleic Acids Res* 2004;32:D109–11.
54. Griffiths-Jones S. miRBase: the microRNA sequence database. *Methods Mol Biol* 2006;342:129–38.
55. Griffiths-Jones S. miRBase: microRNA sequences and annotation. *Curr Protoc Bioinform* 2010;19:1–10. Chapter 12: Unit 12.
56. Griffiths-Jones S, Grocock RJ, van Dongen S, et al. miRBase: microRNA sequences, targets and gene nomenclature. *Nucleic Acids Res* 2006;34:D140–4.
57. Griffiths-Jones S, Saini HK, van Dongen S, et al. miRBase: tools for microRNA genomics. *Nucleic Acids Res* 2008;36:D154–8.
58. Mankame TP, Zhou G, Linggen MW. Identification and characterization of the human NOL7 gene promoter. *Gene* 2010;456:36–44.
59. Illingworth RS, Bird AP. CpG islands—[']A rough guide'. *FEBS Letters* 2009;583:1713–20.
60. Dong SM, Kim HS, Rha SH, et al. Promoter hypermethylation of multiple genes in carcinoma of the uterine cervix. *Clin Cancer Res* 2001;7:1982–6.
61. Zur Hausen H. Papillomaviruses and cancer: from basic studies to clinical application. *Nat Rev Cancer* 2002;2:342–50.
62. Woodman CBJ, Collins SI, Young LS. The natural history of cervical HPV infection: unresolved issues. *Nat Rev Cancer* 2007;7:11–22.
63. Doorbar J. Molecular biology of human papillomavirus infection and cervical cancer. *Clin Sci (Lond)* 2006;110:525–41.
64. Moore DH. Cervical cancer. *Obstet Gynecol* 2006;107:1152–61.
65. Yu KJ, Rader JS, Borecki I, et al. CD83 polymorphisms and cervical cancer risk. *Gynecol Oncol* 2009;114:319–22.
66. Smith-McCune KK, Weidner N. Demonstration and characterization of the angiogenic properties of cervical dysplasia. *Cancer Res* 1994;54:800–4.
67. Dellas A, Moch H, Schultheiss E, et al. Angiogenesis in cervical neoplasia: microvessel quantitation in precancerous lesions and invasive carcinomas with clinicopathological correlations. *Gynecol Oncol* 1997;67:27–33.
68. Davidson B, Goldberg I, Kopolovic J. Angiogenesis in uterine cervical intraepithelial neoplasia and squamous cell carcinoma: an immunohistochemical study. *Int J Gynecol Pathol* 1997;16:335–8.
69. Lee JS, Kim HS, Jung JJ, et al. Angiogenesis, cell proliferation and apoptosis in progression of cervical neoplasia. *Anal Quant Cytol Histol* 2002;24:103–3.
70. Ozalp S, Yalcin OT, Oner U, et al. Microvessel density as a prognostic factor in preinvasive and invasive cervical lesions. *Eur J Gynaecol Oncol* 2003;24:425–8.
71. Ravazoula P, Zolota V, Hatjicondi O, et al. Assessment of angiogenesis in human cervical lesions. *Anticancer Res* 1996;16:3861–64.
72. Triratanachart S, Niruthisard S, Trivijitsilp P, et al. Angiogenesis in cervical intraepithelial neoplasia and early-staged uterine cervical squamous cell carcinoma: clinical significance. *Int J Gynecol Cancer* 2006;16:575–80.
73. Hudelist G, Manavi M, Pischinger KI, et al. Physical state and expression of HPV DNA in benign and dysplastic cervical tissue: different levels of viral integration are correlated with lesion grade. *Gynecol Oncol* 2004;92:873–80.
74. Li W, Wang W, Si M, et al. The physical state of HPV16 infection and its clinical significance in cancer precursor lesion and cervical carcinoma. *J Cancer Res Clin Oncol* 2008;134:1355–61.
75. Duenas-Gonzalez A, Lizano M, Candelaria M, et al. Epigenetics of cervical cancer: an overview and therapeutic perspectives. *Molecular Cancer* 2005;4:38.
76. Suzuki MM, Bird A. DNA methylation landscapes: provocative insights from epigenomics. *Nat Rev Genet* 2008;9:465–76.
77. Lister R, Pelizzola M, Dowen RH, et al. Human DNA methylomes at base resolution show widespread epigenomic differences. *Nature* 2009;462:315–22.
78. Wu H, Coskun V, Tao J, et al. Dnmt3a-dependent non-promoter DNA methylation facilitates transcription of neurogenic genes. *Science* 2010;329:444–8.
79. Choi JK. Contrasting chromatin organization of CpG islands and exons in the human genome. *Genome Biol* 2010;11:R70.
80. Skotheim RI, Nees M. Alternative splicing in cancer: noise, functional, or systematic?. *Int J Biochem Cell Biol* 2007;39:1432–49.
81. Tazi J, Bakkour N, Stamm S. Alternative splicing and disease. *Biochim Biophys Acta* 2009;1792:14–26.
82. Zhou G, Doci CL, Linggen MW. Identification and functional analysis of NOL7 nuclear and nucleolar localization signals. *BMC Cell Biol* 2010;11:74.
83. Gardner LB. Nonsense-mediated RNA decay regulation by cellular stress: implications for tumorigenesis. *Mol Cancer Res* 2010;8:295–308.
84. McGlincy NJ, Smith CW. Alternative splicing resulting in nonsense-mediated mRNA decay: what is the meaning of nonsense? *Trends Biochem Sci* 2008;33:385–93.
85. Roy SW, Irimia M. Intron mis-splicing: no alternative? *Genome Biol* 2008;9:208.
86. Hartmann B, Valcarcel J. Decrypting the genome's alternative messages. *Curr Opin Cell Biol* 2009;21:377–86.
87. Isken O, Maquat LE. Quality control of eukaryotic mRNA: safeguarding cells from abnormal mRNA function. *Genes Dev* 2007;21:1833–56.
88. Scholzova E, Malik R, Sevcik J, et al. RNA regulation and cancer development. *Cancer Lett* 2007;246:12–23.
89. Chatterjee S, Pal JK. Role of 5'- and 3'-untranslated regions of mRNAs in human diseases. *Biol Cell* 2009;101:251–62.
90. Chen JM, Ferec C, Cooper DN. A systematic analysis of disease-associated variants in the 3' regulatory regions of human protein-coding genes I: general principles and overview. *Hum Genet* 2006;120:1–21.
91. Lopez de Silanes I, Quesada MP, Esteller M. Aberrant regulation of messenger RNA 3'-untranslated region in human cancer. *Cell Oncol* 2007;29:1–17.